Communications in Physics, Vol. 35, No. 3 (2025), pp. 289-299

DOI: https://doi.org/10.15625/0868-3166/22724

Role of chitosan in enhancing Raman signal and improving uniformity of paper-based SERS substrate

Nguyen Thi Bich Ngoc † , Nguyen Trong Nghia, Nguyen Thi Thuy, Nguyen Duc Toan and Nghiem Thi Ha Lien

Institute of Physics, Vietnam Academy of Science and Technology, 10 Dao Tan, Giang Vo, 10000 Hanoi, Vietnam

E-mail: †ntbngoc@iop.vast.vn

Received 18 April 2025 Accepted for publication 6 August 2025 Published 16 September 2025

Abstract. Chitosan, a naturally occurring polysaccharide extracted from crustacean shells, was utilized as a functional additive in the fabrication of Surface Enhanced Raman Scattering (SERS) substrates featuring silver bar-like nanostructures aligned on the paper surface via a direct chemical reduction approach. As a coupling agent, chitosan enhances the interaction between silver ions and cellulose fibers through chemical interactions between [Ag(chitosan)]⁺ complexes and surface hydroxyl (–OH) groups on the cellulose substrate. Thanks to this interaction, silver nanostructures are better adsorbed and more uniformly distributed on the surface of the filter paper. In the presence of chitosan, the resulting silver nanostructures adopt well-defined, bar-like morphologies aligned along the cellulose fibers, in stark contrast to the disordered and scattered structures observed in its absence. The effect of chitosan on the optical properties and SERS performance of the substrates was thoroughly examined. The analyte used to evaluate SERS activity was melamine, a nitrogen-rich compound often used as a food adulterant. Results demonstrate that chitosan notably improves both the enhancement factor (EF) and the signal uniformity of the paper-based SERS substrates, highlighting its dual role as a structural modulator and stabilizer for silver nanostructure growth.

Keywords: chitosan; silver nanostructures; cellulose fibers; surface enhanced Raman scattering (SERS); paper-based SERS substrates.

Classification numbers: 81.05.Bx; 78.30.-j; 78.68.+m.

1. Introduction

Surface-enhanced Raman scattering (SERS) has become an effective technique for detecting chemical and biological species due to its high sensitivity and ability to distinguish molecular structures via characteristic spectral features [1–4]. The performance of a SERS substrate in terms of sensitivity, reproducibility, and stability is predominantly dictated by its structural design, including the choice of plasmonic material and the architecture of the nanoparticle-binding support matrix [4]. Additionally, the intended application critically influences the fabrication strategy. For in situ analysis, particularly when combined with portable Raman systems or smartphone-based detectors, the development of SERS substrates requires fabrication methods that are rapid, cost-efficient, and technically simple. Flexible SERS substrates have thus received increasing attention, as they enable direct sampling from irregular surfaces and allow non-invasive measurements without complex pretreatment [5,6]. Among various flexible materials, paper is a widely used substrate due to its porous structure, mechanical flexibility, low cost, biocompatibility, and environmental compatibility [4,7].

Efficient in situ SERS applications require substrates that are cost-effective, rapidly fabricated, and structurally compatible with direct integration. The direct chemical reduction method addresses these demands by enabling the in-situ synthesis of plasmonic nanostructures on paper substrates, bypassing the use of pre-formed nanoparticles. In this approach, the physicochemical interaction between metal ions and the cellulose matrix plays a key role in determining the characteristics of the resulting SERS-active surface [8,9]. Paper, primarily composed of cellulose fibers, consists of linear chains of D-glucose units connected by $\beta - (1 \rightarrow 4)$ glycosidic linkages. Its high crystallinity, arising from intramolecular hydrogen bonding among hydroxyl groups, restricts metal ion adsorption by limiting the accessibility of reactive sites [10, 11]. To overcome this, surface modification techniques have been employed to enhance chelating ability. Among these, copolymerization with functional monomers prior to reduction has been shown to significantly improve metal ion affinity, promoting the formation of dense, uniform nanostructures on the paper surface [12, 13].

Chitosan, a naturally abundant polysaccharide with a molecular structure like that of cellulose, has been extensively employed to modify paper substrates for SERS applications. In weakly acidic environments, chitosan behaves as a cationic polyelectrolyte due to the protonation of its amino groups in the molecular backbone [4,10]. Since 2009, Varsha Thomas and co-workers have demonstrated the strong metal ion adsorption capacity of chitosan, attributed to its pronounced chelating ability toward heavy metals [14]. In the fabrication of paper-based SERS substrates via direct chemical reduction, chitosan has been widely introduced to enhance silver ion retention. For example, Ahmad et al. coated cellulose fibers with chitosan prior to NaBH₄ reduction, resulting in improved Ag⁺ adsorption [15]. Similarly, Kang's group pretreated cellulose with chitosan and NaOH, not only enhancing mechanical and thermal stability but also yielding substrates with improved hydrophobicity, signal uniformity, and reproducibility 7,16. Like the approach reported by Kim et al. (2025), chitosan was employed as a surface modifier to pre-treat the paper substrate, improving the uniformity and reproducibility of the SERS signals [16]. Dan Li's group compared two strategies: chitosan pretreatment versus direct deposition of Ag-chitosan complexes. The pretreatment approach achieved superior performance, detecting melamine down to 1 mg/L [17]. In our recent study (2023), we adopted a similar strategy by directly reducing Ag-chitosan complexes

on filter paper. The resulting substrates exhibited performance comparable to those fabricated via pretreatment, achieving a significantly lower detection limit of 10-8 M [9].

In this work, the role of chitosan as a bridging agent between silver ions and cellulose fibers is further explored, attributed to its strong affinity arising from interactions between Agchitosan complexes and surface hydroxyl (–OH) groups of cellulose. Silver nanostructures with anisotropic morphology were synthesized via chemical reduction using a glucose solution under continuous stirring. The effect of chitosan incorporation on the enhancement factor (EF) and signal uniformity of the paper-based SERS substrates was systematically investigated by directly comparing with control substrates prepared without chitosan.

2. Experiment

2.1. Reagents and materials

For this work, chitosan ($C_{56}H_{103}N_9O_{39}$, deacetylated chitin, low molecular weight), silver nitrate (AgNO₃, 99%), citric acid ($C_6H_8O_7$, 99.5%), glucose ($C_6H_{12}O_6$, 99.5%), and melamine ($C_3H_6N_6$, 99%) were obtained from Sigma Aldrich. The standard laboratory Whatman filter paper (#3, 6 μ m, thickness 0.39 μ m) was obtained from GE Healthcare companies in the UK. Deionized water (resistance > 1 M Ω) was used to prepare paper-based SERS substrates and aqueous solutions of the analytes.

2.2. Preparation of paper-based SERS substrates

The experimental processes of paper-based SERS substrates without chitosan (PSERS) and paper-based SERS substrates using chitosan (PSERS-CH) are shown in the schematic diagram (Fig. 1).

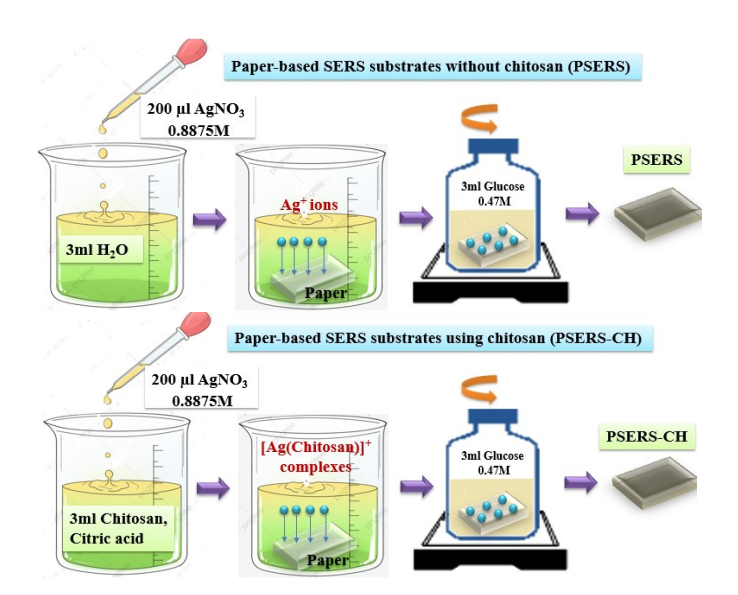


Fig. 1. The synthesis procedure of paper-based SERS substrates without chitosan and using chitosan.

Preparation of paper Ag^+ ions: The filter paper (1.2 cm \times 1.2 cm) was immersed in 3 ml of H_2O and 200 μ l of $AgNO_3$ 0.8875 M solution for 24 h at room conditions to adsorb Ag^+ ions on cellulose fibers.

Preparation of paper – [Ag(Chitosan)]⁺ complexes: The chitosan solution was fabricated by chitosan (10% wt) and citric acid (10% wt) in H₂O in 24 h under room conditions. After that, the chitosan solution was removed from the excess residue using a membrane filter with a pore size of 450 nm. To form the [Ag(Chitosan)]⁺ complexes solution, 3 ml of the chitosan solution and 200 μl of AgNO₃ 0.8875 M were mixed at room temperature for 2 hours. The paper strips, measuring 1.2 cm x 1.2 cm, were immersed in a solution of [Ag(Chitosan)]⁺ complexes for 24 hours at room temperature to adsorb onto the cellulose fibers. Then, the paper – Ag⁺ ions and the paper - [Ag(Chitosan)]⁺ were reduced by reducing agent solution, including 3 ml glucose, 0.47 M, and NaOH in 1 min under a stirring speed of 2000 round/min. The color change of PSERS and PSERS-CH was observed from white to dark green. However, the paper-based SERS substrates using chitosan had darker colors. The SERS substrates are washed with deionized water to remove residue and dried in room temperature. Finally, these substrates are stored at 4°C and in a vacuum.

2.3. Characterization methods

The morphology and distribution of silver nanostructures on paper have been characterized by a Scanning Electron Microscopy (SEM, Hitachi S-4800). The optical spectra of the PSERS were recorded using Ultraviolet–Visible Spectroscopy (JASCO-V570-UV-Vis-NIR). Raman spectra were acquired using a Raman spectroscope (Labram HR Evolution). The elemental analysis measurements were performed using an Energy Dispersive X-ray Spectrometer (EDS) attached with a Hitachi Regulus 8100 Field-Emission Scanning Electron Microscope.

2.4. SERS measurements

Ten microliters of the melamine solution with different concentrations were dropped onto paper-based SERS substrates (size 3×3 mm) and allowed to dry in air. The SERS activity was measured using a Raman spectrograph with an excitation wavelength of 633 nm, a laser output of 10 mW, an acquisition time of 3 s, and a laser spot size of 14 μ m.

3. Results and discussion

3.1. Impact of chitosan on the characteristics of paper-based SERS substrates

The surface morphologies of PSERS-CH and PSERS substrates were systematically characterized using SEM, as presented in Fig. 2. In the case of PSERS-CH (Fig. 2a), silver nanostructures are uniformly distributed on the surface of the paper fibers, forming a dense and continuous layer. At higher magnifications, these nanostructures exhibit a well-defined bar-like morphology, radially arranged into flower-like structures with homogeneous size and shape. In contrast, the PSERS sample without chitosan (Fig. 2b) shows a markedly different morphology. The silver nanostructures are irregularly distributed, primarily forming aggregated rod-like clusters with heterogeneous sizes and shapes. Additionally, a small number of spherical silver nanoparticles with diameters of approximately 30 nm are sparsely distributed on both the paper surface and the rod silver structure. Compared to PSERS, the PSERS-CH substrate exhibits not only a higher density of silver nanostructures but also significantly greater structural thickness. These observations

suggest that chitosan plays a critical role in promoting the uniform deposition and morphological control of silver nanostructures on paper-based substrates.

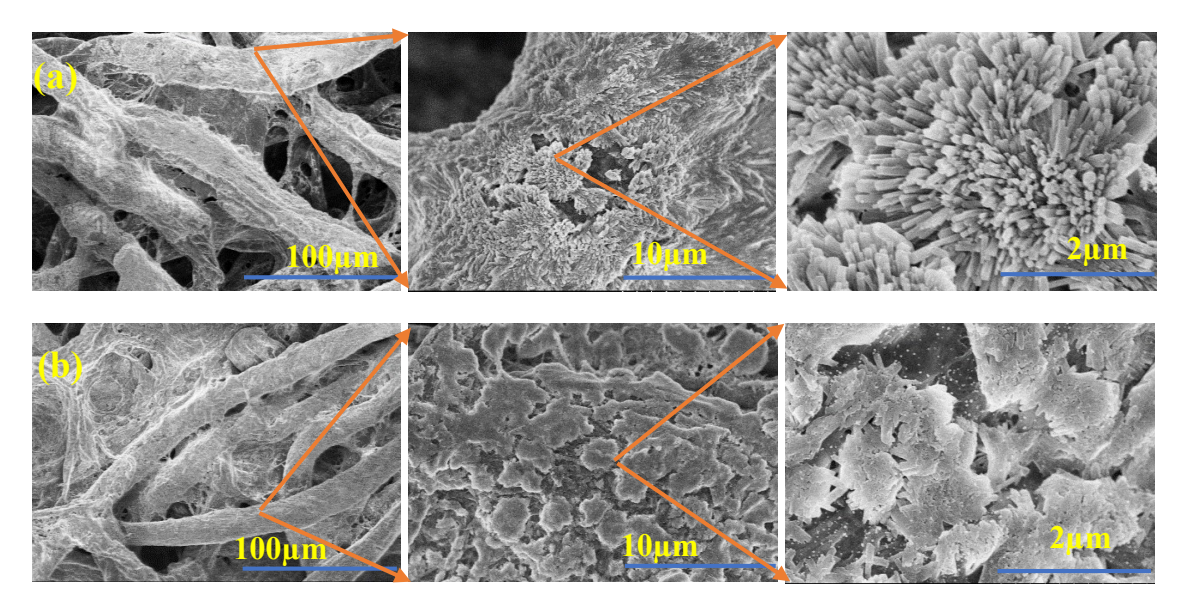


Fig. 2. SEM images of PSERS-CH (a) and PSERS (b) at different resolutions.

This difference can be attributed to the dual role of chitosan as both a stabilizing agent and a promoter for silver ion adsorption on the surface of cellulose fibers. The molecular structure of chitosan contains amino (-NH₂) and hydroxyl (-OH) functional groups, which enable it to function as a chelating polymer with high adsorption capacity for various metal ions [14]. During the initial stage of the fabrication process, the amino groups in chitosan act as ligands or binding sites for silver ions, forming stable complexes, as illustrated in the accompanying scheme:

$$Ag^+ + Chitosan \rightarrow [Ag(chitosan)]^+$$
.

The silver–chitosan complexes are anchored onto the cellulose fibers of the paper substrate through interactions with surface hydroxyl (–OH) functional groups. These hydroxyl groups on the cellulose fibers coordinate with silver–chitosan complexes containing multiple silver ions, thereby significantly enhancing silver ion adsorption onto the cellulose matrix. This increased adsorption capacity is attributed to the cooperative interaction between chitosan and cellulose functional groups. Consistent with these observations, previous studies have reported that in the absence of chitosan, the adsorption capacity of silver ions on cellulose fibers is markedly reduced [18–20].

During the reduction of silver ions into silver nanostructures, spherical silver seed nanoparticles are initially formed. In the presence of glucose as a reducing agent, these silver seeds preferentially grow along the (111) crystallographic planes, subsequently evolving into rod-shaped silver nanostructures on the cellulose fibers under continuous stirring. Notably, the silver–chitosan complexes exhibit stronger binding affinity to the functional groups on the cellulose fiber surfaces than free silver ions, resulting in their uniform immobilization on the paper substrate without being

detached during the stirring process. Furthermore, chitosan functions as a capping agent, contributing to the stabilization and alignment of the silver nanorods along the cellulose fibers, as illustrated in Fig. 2a.

In contrast, in the absence of chitosan, the interactions between silver ions and the functional groups on cellulose fibers are insufficiently strong to retain all silver species during stirring. Consequently, a portion of the silver ions is lost, leading to the formation of discrete and non-uniform silver nanostructures after glucose reduction. These structures, comprising a mixture of rod-like and spherical shapes, display random and disordered distribution on the cellulose fiber surface (Fig. 2b). This behavior is attributed to the detachment and migration of silver seed nanoparticles from the filter paper under stirring conditions, coupled with the absence of stabilizing surfactants to control and maintain the structural organization.

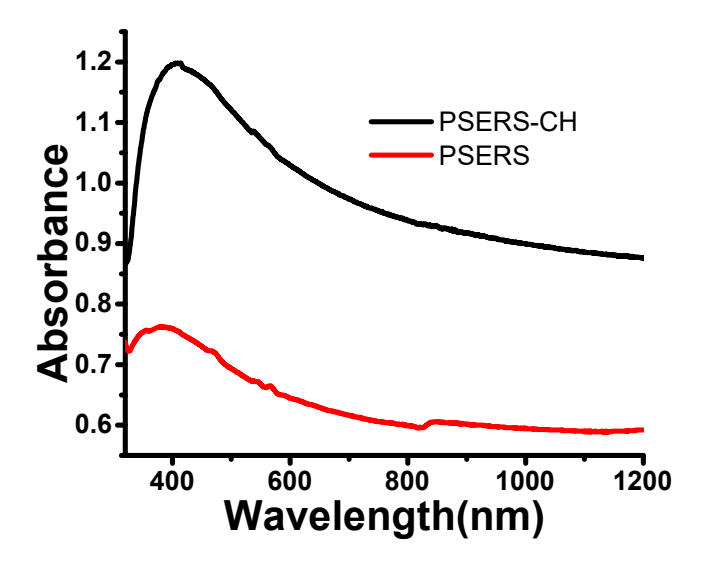


Fig. 3. UV-visible diffuse reflectance spectra of PSERS and PSERS-CH.

The increase in the number of silver nanostructures formed on cellulose fibers by using chitosan is also clearly shown in the UV-visible diffuse reflectance spectra of PSERS and PSERS-CH (Fig. 3). Both samples have relatively similar diffuse reflectance spectra with a peak at about 400 nm, a universal spectrum rising and almost a straight line on the long wavelengths. Plasmon structures with diffuse reflectance spectra are often used for SERS applications because they are compatible with many laser excitation sources. However, the absorbance using chitosan substrates is about 1.6 times higher than without chitosan substrates. This also proves that the number of silver structures on the PSERS-CH paper is greater than that of PSERS.

The elemental compositions of the PSERS and PSERS-CH substrates were further analyzed using EDS, as summarized in Table 1. Both types of substrates contain carbon, oxygen, and silver elements. The presence of carbon and oxygen is attributed to the cellulose fibers of the paper substrate. However, notable differences in the elemental mass percentages, particularly for silver (Ag), were observed between PSERS and PSERS-CH. Specifically, the PSERS-CH substrate exhibits a silver content of 28.48 %, approximately 1.8 times higher than that of the PSERS

substrate, which contains 15.74 % silver. The increased silver content in the PSERS-CH substrate indicates a greater amount of silver nanostructures deposited on the paper fibers, facilitated by the presence of chitosan. These findings are in good agreement with the SEM observations and UV–visible diffuse reflectance spectra results.

Table 1. PSERS and PSERS-CH substrates compositions (wt.%) are characterized by optical emission spectroscopy.

Sample	С	О	Ag
PSERS	37.51	46.75	15.74
PSERS-CH	28.99	42.53	28.48

3.2. Impact of chitosan on SERS characteristic of paper-based SERS substrates

The influence of chitosan on the SERS performance was evaluated using melamine as a model analyte. The SERS spectra of melamine adsorbed on PSERS and PSERS-CH substrates at varying molar concentrations ranging from 10-4 to 10-8 M are presented in Fig. 4 (a, c). A peak at 695 cm-1, corresponding to the ring-breathing vibration mode of melamine molecules [9], was observed on both PSERS and PSERS-CH substrates. Notably, this characteristic peak exhibits a red shift compared to the Raman spectrum of melamine powder on paper, as shown in Fig. 5 and Table 2. In our previous study, this shift was attributed to the interaction between melamine molecules and the silver nanostructures on the substrate surface [9].

The Raman spectra presented in Fig. 4, further confirm that both PSERS and PSERS-CH substrates exhibit high detection sensitivity. The detection limits for melamine molecules on PSERS and PSERS-CH substrates were determined to be 10^{-6} M and 10^{-7} M, respectively.

Table 2. Raman signal intensity of melamine on paper, PSERS and PSERS substrates.

Substrates	Characteristic peak of melamine (cm ⁻¹)	Detection limits (M)	Intensity (a.u.)
Paper	680	_	3459
PSERS-CH	695	10^{-7}	4958
PSERS	695	10^{-6}	4100

To quantify the enhancement of the Raman signal of PSERS and PSERS-CH substrates, we calculated the analytical EF for detecting melamine according to the equation [9]:

$$EF = \left(\frac{I_{SERS}}{I_{Raman}}\right) \left(\frac{N_{Raman}}{N_{SERS}}\right). \tag{1}$$

Here, I_{SERS} and I_{Raman} (3459 au from Fig. 5) are the intensities of the characteristic bands in the SERS and Raman spectra, respectively; N_{SERS} and N_{Raman} represent the estimated number of melamine molecules probed for a bulk sample (melamine powder on paper) and on the surface of

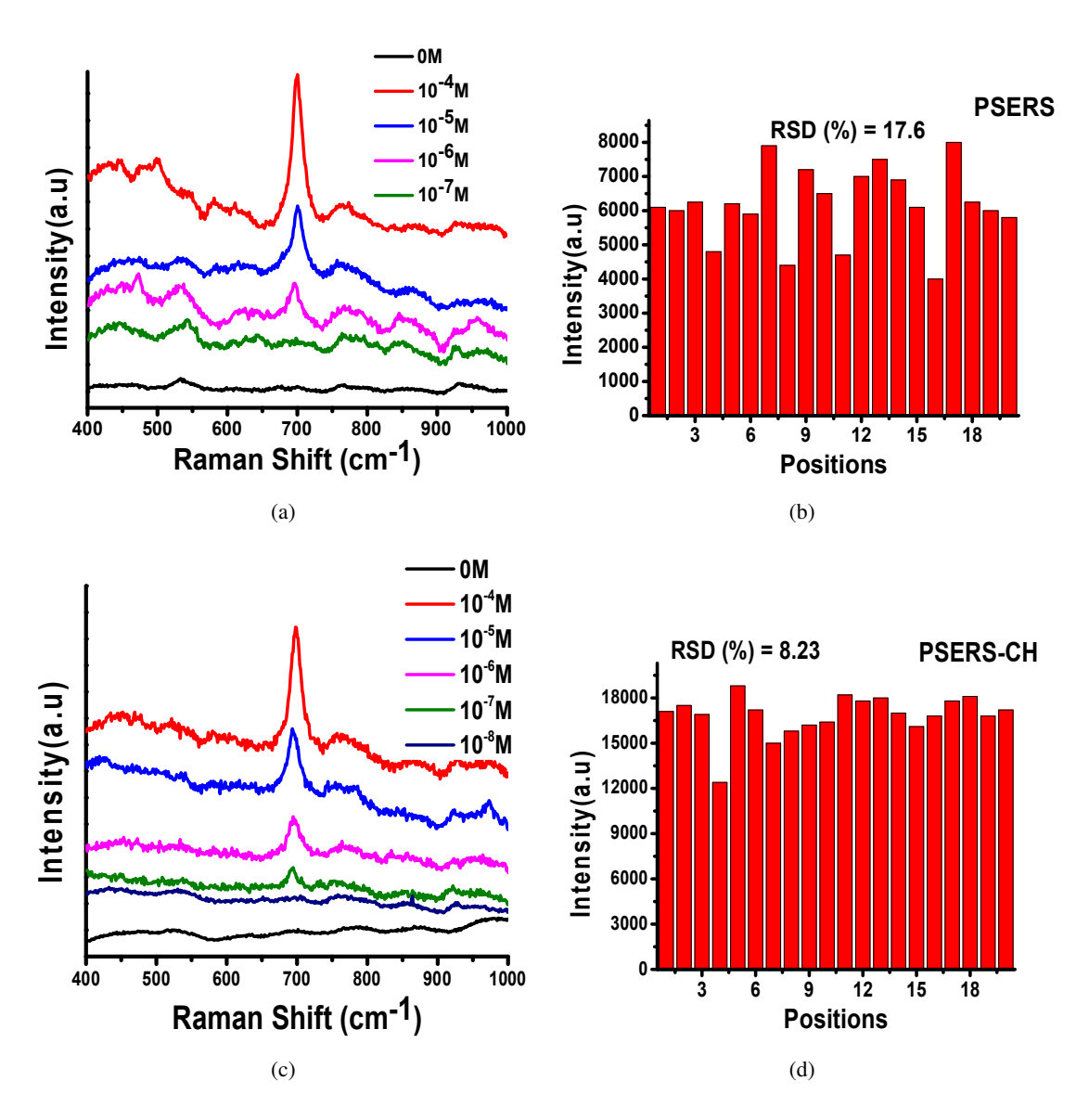


Fig. 4. The detection limit for melamine on PSERS (a) and PSERS-CH (c) substrates. The peak intensity at 695 cm⁻¹ of melamine 10⁻⁴M concentration at 20 random points in PSERS (b) and PSERS-CH (d) substrates.

SERS substrates. They are calculated according to the following formula [9]:

$$N_{SERS} = \eta N_A V C_{SERS} \frac{V_{laser}}{V_{SERS}}, \tag{2}$$

$$N_{Raman} = N_A \frac{d_{Melamine}}{M} V_{laser}, \tag{3}$$

$$\frac{N_{Raman}}{N_{SERS}} = \frac{d_{Melamine}V_{SERS}}{\eta MVC_{SERS}}.$$
 (4)

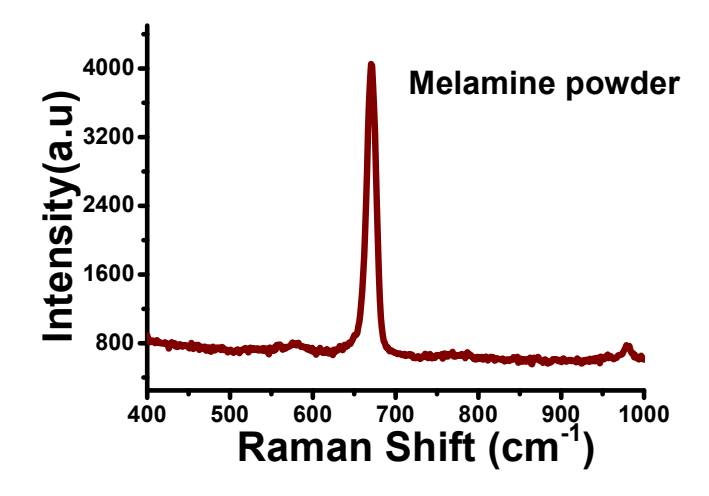


Fig. 5. Raman spectrum of the melamine powder was measured on paper.

Here, N_A is the Avogadro number, V is the total volume of melamine solution drop on the SERS substrates (10 μ L), V_{laser} is the volume of the laser, V_{SERS} (3.51 × 10⁻⁹ m³) is the total volume of the SERS substrate covered by the drop of melamine solution (3 mm × 3 mm × 0.39 mm), $d_{melamine} = 1547 \text{ kg/m}^3$ is the density of melamine. M (126.12 g/mol) is the molar mass of melamine. η is the total active volume, with SERS accounting for the total volume of the laser spot [9]. SEM images of the PSERS-CH substrate (Fig. 1a) and PSERS (Fig. 1c) showed that the area of silver nanostructures covering the filter paper fibers accounted for approximately 95% (η =0.95) and 75% (η =0.75), respectively.

The calculated EF of PSERS and PSERS-CH substrates are estimated as shown in Table 3. The estimated EF confirmed that the paper-based SERS substrates using chitosan improved the quality of the enhancement effect. The EF of this substrate is one step higher than the PSERS substrate. The characteristics of silver nanoparticles on paper fibers are the most critical conditions that affect the Raman enhancement effect. The number of distributed hot spots of PSERS-CH is attributed to the tips and the narrow gaps of the rod-shaped silver nanostructures.

Additionally, the dense distribution of silver nanostructures covering the paper fibers of the PSERS-CH substrate also increases the number of hot spots. All these features are the reason why these SERS substrates give higher EF than PSERS substrates. In addition, the distribution of silver nanostructures on paper fibers also affects the uniformity of the SERS signal.

Table 3. The EF of paper-based SERS substrates.

SERS substrates	I _{SERS} (au)	C_{SERS} (M)	η	EF
PSERS PSERS-CH	4100 4958	$10^{-6} \\ 10^{-7}$	0.,0	3.4×10^8 3.2×10^9

To evaluate the signal uniformity of SERS substrates, the relative standard deviation (RSD) was calculated for twenty distinct spots (n=20) of 10 μ l melamine at a concentration of 10⁻⁴ M

atrazine deposited on the PSERS (Fig. 4b) and PSERS-CH (Fig. 4d) substrates, which is described with the following equation [9]:

$$SD = \sqrt{\frac{\sum_{i=1}^{n} (x_i - \bar{x})^2}{n-1}}, \qquad RSD = \frac{SD}{\bar{x}} \times 100 \, (\%).$$
 (5)

Here, SD is the standard deviation, x_i denotes the Raman signal intensity at 700 cm⁻¹ at the i th time of melamine, and \bar{x} implies the average Raman signal intensity [9]. The RSD values of PSERS and PSERS-CH substrates obtained in this experiment were approximately 17.6% and 8.23%, respectively. The RSD value shows that the SERS signal uniformity of the PSERS-CH substrate is higher than that of the PSERS substrate. This is the result of the fact that, thanks to the effect of chitosan, the silver nanostructures were formed and distributed evenly on the paper fibers.

4. Conclusion

In summary, Chitosan notably enhances the properties of paper-based SERS substrates produced via direct chemical reduction. Its presence promotes the formation of orderly, rod-shaped silver nanostructures that are more uniformly and densely distributed on the paper fibers. Chitosan facilitates stronger adhesion of silver nanostructures by enabling bonding between silver ions and the cellulose in the filter paper. As a result, PSERS-CH substrates exhibit lower detection limits or higher enhancement factors (EF) compared to PSERS, along with significantly improved signal uniformity.

Acknowledgments

This study was supported by Vietnam Academy of Science and Technology (VAST) with grant number VAST01.02/25-26. We are also grateful for the use of the facilities of the Joint Optics Laboratory between IOP and GUST, VAST.

Authors contributions

Nguyen Thi Bich Ngoc: Writing, Methodology. Nguyen Thi Thuy: Formal analysis. Nguyen Trong Nghia and Nguyen Duc Toan: Measurement. Nghiem Thi Ha Lien: Formal analysis and Review.

Conflict of interest

The authors declare no conflicts of interest.

References

- [1] C. Puente, M. S. Domínguez, C. L. Brosseau and I. López, Silver-chitosan and gold-chitosan substrates for surface-enhanced raman spectroscopy (sers): Effect of nanoparticle morphology on sers performance, Mater. Chem. Phys. 260 (2021) 124107.
- [2] K. Yan, F. Xu, W. Wei, C. Yang, D. Wang and X. Shi, *Electrochemical synthesis of chitosan/silver nanoparticles multilayer hydrogel coating with ph-dependent controlled release capability and antibacterial property*, Colloids Surf. B Biointerfaces **202** (2021) 111711.
- [3] O. E. Eremina, O. O. Kapitanova, E. A. Goodilin and I. A. Veselova, Silver-chitosan nanocomposite as a plasmonic platform for sers sensing of polyaromatic sulfur heterocycles in oil fuel, Nanotechnology 31 (2020) 225503.

- [4] N. C. T. Martins, S. Fateixa and T. Trindade, *Chitosan coated papers as sustainable platforms for the development of surface-enhanced raman scattering hydrophobic substrates*, J. Mol. Liq. 375 (2023) 121388.
- [5] S. Yi, M. Yang, Y. Yu, Z. Li, D. Zhang, F. Han et al., Highly sensitive flexible sers substrates with a sandwich structure for rapid detection of trace pesticide residues, Appl. Surf. Sci. 654 (2024) 159455.
- [6] Q. Hu, D. Yang, J. He, M. Han and C. Zhang, Femtosecond laser-induced sub-wavelength periodic structure for nano-transfer of pdms flexible sers substrate, Opt. Mater. 153 (2024) 115597.
- [7] Y. Kang, H. J. Kim, S. H. Lee and H. Noh, *Paper-based substrate for a surface-enhanced raman spectroscopy biosensing platform-a silver/chitosan nanocomposite approach*, Biosensors 12 (2022) 266.
- [8] D. Das, S. Senapati and K. K. Nanda, "rinse, repeat": An efficient and reusable sers and catalytic platform fabricated by controlled deposition of silver nanoparticles on cellulose paper, ACS Sustain. Chem. Eng. 7 (2019) 14089.
- [9] N. T. B. Nguyen, T. T. Nguyen, N. T. Nguyen, T. D. Nguyen, H. Q. Do, H. V. Chu et al., Multi-shape silver nanoparticles on filter paper by the chemical reduction method, J. Nanopart. Res. 25 (2023) 126.
- [10] J. Yang, G. J. Kwon, K. Hwang and D. Y. Kim, Cellulose-chitosan antibacterial composite films prepared from libr solution, Polymers 10 (2018) 1058.
- [11] T. Kamal, S. B. Khan, S. Haider, Y. G. Alghamdi and A. M. Asiri, Thin layer chitosan-coated cellulose filter paper as substrate for immobilization of catalytic cobalt nanoparticles, Int. J. Biol. Macromol. 104 (2017) 56.
- [12] A. Hebeish, S. Farag, S. Sharaf and T. I. Shaheen, Development of cellulose nanowhisker-polyacrylamide copolymer as a highly functional precursor in the synthesis of nanometal particles for conductive textiles, Cellulose 21 (2014) 3055.
- [13] M. F. Mohamed, H. A. Essawy, N. S. Ammar and H. S. Ibrahim, Potassium fulvate-modified graft copolymer of acrylic acid onto cellulose as efficient chelating polymeric sorbent, Int. J. Biol. Macromol. 94 (2017) 771.
- [14] V. Thomas, M. M. Yallapu, B. Sreedhar and S. K. Bajpai, Fabrication, characterization of chitosan/nanosilver film and its potential antibacterial application, J. Biomater. Sci. Polym. Ed. 20 (2009) 2129.
- [15] I. Ahmad, T. Kamal, S. B. Khan and A. M. Asiri, An efficient and easily retrievable dip catalyst based on silver nanoparticles/chitosan-coated cellulose filter paper, Cellulose 23 (2016) 3577.
- [16] R. Akter, T. Kim, J. S. Choi and H. Kim, A new chitosan-modified paper-based sers glucose sensor with enhanced reproducibility, stability, and sensitivity for non-enzymatic label-free detection, Biosensors 15 (2025) 153.
- [17] D. Li, D. Y. Lv, Q. X. Zhu, H. Li, H. Chen, M. M. Wu et al., Chromatographic separation and detection of contaminants from whole milk powder using a chitosan-modified silver nanoparticles surface-enhanced raman scattering device, Food Chem. 224 (2016) 382.
- [18] D. Zhou, L. Zhang, J. Zhou and S. Guo, Cellulose/chitin beads for adsorption of heavy metals in aqueous solution, Water Res. 38 (2004) 2643.
- [19] T. M. Mututuvari and C. D. Tran, Synergistic adsorption of heavy metal ions and organic pollutants by supramolecular polysaccharide composite materials from cellulose, chitosan and crown ether, J. Hazard. Mater. **264** (2014) 449.
- [20] S. C. Yang, Y. Liao, K. G. Karthikeyan and X. J. Pan, Mesoporous cellulose-chitosan composite hydrogel fabricated via the co-dissolution-regeneration process as biosorbent of heavy metals, Environ. Pollut. 286 (2021) 117324.